Proceedings of the 11th Brazilian Congress of Thermal Sciences and Engineering -- ENCIT 2006
Braz. Soc. of Mechanical Sciences and Engineering -- ABCM, Curitiba, Brazil,- Dec. 5-8, 2006

Paper CIT06-0395

MATHEMATICAL MODELING AND NUMERICAL SIMULATION OF A THREE-DIMENSIONAL FLOW OVER COMPLEX GEOMETRIES USING THE IMMERSED BOUNDARY METHOD

João Marcelo Vedovoto
Faculty of Mechanical Engineering - Federal University of Uberlândia
João Naves de Ávila Av. 2121,Uberlândia, MG, Brazil
jmvedovoto@mecanica.ufu.br

Rubens Campregher
Department of Mechanical Engineering - Dalhousie University
A1B 3X5 - Halifax, NS - Canada
rubenscamp@dal.ca

Aristeu da Silveira Neto
Faculty of Mechanical Engineering - Federal University of Uberlândia
João Naves de Ávila Av. 2121,Uberlândia, MG, Brazil
aristeus@mecanica.ufu.br

Abstract. *The mathematical modeling and numerical simulation of real problems in engineering has a fundamental importance. However, the search for accurate and viable solutions constitutes in a great challenge.*
The goal of this paper is to present the Immersed Boundary methodology for modeling and simulating flows over complex three-dimensional geometries, and also characterize the generation of wingtip vortices. This methodology is being developed in the Laboratory of Heat and Mass Transfer and Fluid Dynamics (LTCM).
The Immersed Boundary method uses two independent domains in the solution of the flows over complex geometries: An Eulerian domain, which is discretized using Finite Volume Method over a non-uniform mesh to integrate the Navier-Stokes equations, and a second-order approximation for time and space derivatives. The Lagrangian domain is represented by a superficial unstructured mesh, composed by triangles.
The in-house parallel code runs on a Beowulf-class cluster, a viable and reliable alternative to solve problems that demand very large computational resources. Three-dimensional flow over airfoils NACA-0012 were simulated aiming to accurately study wingtip vortices. The results present a good agreement with literature, and it is possible to understand the generation and development of the vortices.

Keywords. Immersed Boundary Method, Virtual Physical Model, complex geometries, wingtip vortices.

1. Introduction

When an aircraft wing generates lift, it also produces horizontal, tornado-like vortices that create a potential wake-vortex hazard problem for other aircraft trailing. The powerful, high-velocity airflows contained in the wake behind the generating aircraft are long-lived, invisible, and a serious threat to aircraft encountering the system, especially small aviation aircraft. Thus the understanding of such phenomenon is fundamental.

In present work the Immersed Boundary method is used to simulate the conditions of generation and decay of those wingtip vortices. An in-house parallel code running on a Beowulf-class cluster is used.

In the Immersed Boundary (IB) methods, the presence of a solid or a gaseous interface inside a flow can be simulated by adding a source term into the Navier-Stokes equations, acting as a fluid body force. The way that this force is evaluated differentiates the methodologies among them. Furthermore, an important characteristic presented by the Immersed Boundary methodologies is that the immersed obstacle can be represented by a Lagrangian mesh while the flow domain can be discretized by an Eulerian grid such as Cartesian or cylindrical. There are, also, an interpolation function that promotes the information transfer from one domain to another. This domain independence allows one to promote the immersed body a displacement and/or a deformation relative to the flow grid.

The development of the Immersed Boundary method was credited to Charles Peskin and his collaborators, aiming to simulate the blood flow through cardiac valves. Accordingly to Peskin's work (Peskin, 1977), the source of the additional force term was due to the elastic boundary deformation rate, in which their constitutive points were tied by elastic membranes

More recently, Lima e Silva (Lima e Silva *et al*, 2003) proposed a model that evaluates the force field by the momentum equation based on a three points scheme, similar to Mohd-Yusof's (Mohd-Yusof's,1997) work, but using more simplified interpolation schemes that requires less computing resources. Since the model employs momentum equation and model the no-slip condition on the geometry wall in an indirect manner, the model has been called Virtual

Physical Model (VPM) (Lima e Silva *et al,* 2003). This current work proposal is to present an extension to three-dimensional domains of the VPM (Campregher, 2005) and apply it to the flow around a NACA- 0012 airfoil.

2. Mathematical and numerical modeling

The Immersed Boundary method uses two distinct domains to evaluate a flow over a complex geometry. An Eulerian domain is used to describe the behavior of the mean flow and covers the entire flow domain. For its turn, the Lagrangian domain is used to represent the interface fluid/fluid or fluid/solid.

This is one of the great advantage attributed to Immersed Boundary methods since it is possible to simulate flow around complex geometries using a more simplified Eulerian formulation for the fluid and a Lagrangian more versatile and simple grid for the interface fluid/solid. The coupling between Eulerian and the Lagrangian domains is done by Virtual Physical Model (Lima e Silva et al 2003).

In this work, Cartesian meshes were used to discretize the flow domain, configuring a simple and easy implementation, and at low computational cost. The following describes both domains in more details.

2.1. The Eulerian Domain

The domain was discretized by Finite Volume method over a structured non-uniform mesh. The flow is considered incompressible and isothermal. The integral form of the Navier-Stokes for such assumptions becomes:

$$\frac{\partial}{\partial t}\int_{\Omega}\rho\phi d\Omega+\int_{S}\rho\phi\mathbf{v}\cdot n\,dS=\int_{S}\Gamma\nabla\phi\cdot n\,dS+\int_{\Omega}q_{\phi}d\Omega, \tag{1}$$

where ϕ is a property being transported, q_{ϕ} is the term of generation or destruction of ϕ, and Γ^{ϕ} is the diffusivity of ϕ.

The time derivative was approximated by a second-order three-time level (Ferziger & Peric, 2002), and the spatial derivatives by the Central-Difference Scheme.

The pressure-velocity coupling was done by the SIMPLEC method (Van Doormal e Raithby, 1984), with no relaxation in the velocity components equation. A co-located arrangement of variables was employed, and the Rhie-Chow (Rhie-Chow, 1983) interpolation method was used to avoid numerical oscillation due to pressure checkerboard fields.

The linear system originated from the velocity components discretization was solved by the SOR method. The SIP algorithm was used to solve the linear system generated by the discretization of the pressure correction equation.

The time and space integration of equation (1) over an elementary volume, shown in figure (1), after some mathematical arrangements leads to the following equation :

$$\begin{aligned}&\left(\frac{3\phi_p^n-4\phi_p^{n-1}+\phi_p^{n-2}}{2\Delta t}\right)\Delta x\Delta y\Delta z+\left(\rho_e u_e\phi_e-\rho_w u_w\phi_w\right)^n\Delta y\Delta z+\left(\rho_n u_n\phi_n-\rho_s u_s\phi_s\right)^n\Delta x\Delta z+\\&\left(\rho_t u_t\phi_t-\rho_b u_b\phi_b\right)^n\Delta x\Delta y=\left[\left(\Gamma^{\phi}\frac{\partial\phi}{\partial x}\right)_e-\left(\Gamma^{\phi}\frac{\partial\phi}{\partial x}\right)_w\right]^n\Delta y\Delta z+\\&\left[\left(\Gamma^{\phi}\frac{\partial\phi}{\partial y}\right)_n-\left(\Gamma^{\phi}\frac{\partial\phi}{\partial y}\right)_s\right]^n\Delta x\Delta z+\left[\left(\Gamma^{\phi}\frac{\partial\phi}{\partial z}\right)_t-\left(\Gamma^{\phi}\frac{\partial\phi}{\partial z}\right)_b\right]^n\Delta x\Delta y+q_{\phi}\Delta x\Delta y\Delta z\end{aligned}, \tag{2}$$

The first term of the left-hand side of the equation (2) represents the discretization of the transient term by the *three-time level scheme* (Muzaferija and Peric, 1997). This scheme is a second order accurate in time.

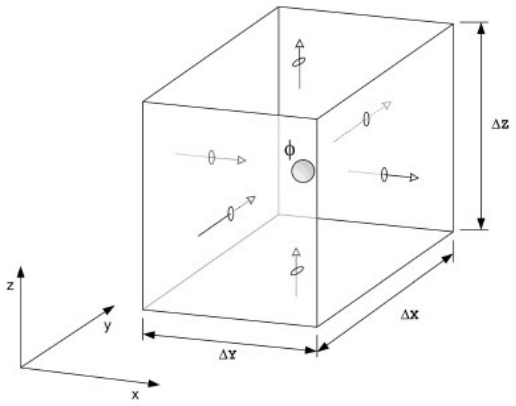

Figure 1: Elementary control volume, with variable ϕ placed on centroid.

2.2. The Lagrangian domain

The Lagrangian approach for analyzing the movement of a particle constitutes of placing a system of coordinates at the particle and follow it individually. In other words, the system of coordinates moves through the flow following the particle. Thus, at each time step the particle keeps its own system of coordinates relatively to a global system of coordinates.

In the Virtual Physical model the geometry to be simulated is characterized by a Lagrangian set of points (see. Fig. (2)). This methodology permits to take advantage of the Lagrangian approximations like the ability to simulate moving bodies by just applying translation operations to the set of points.

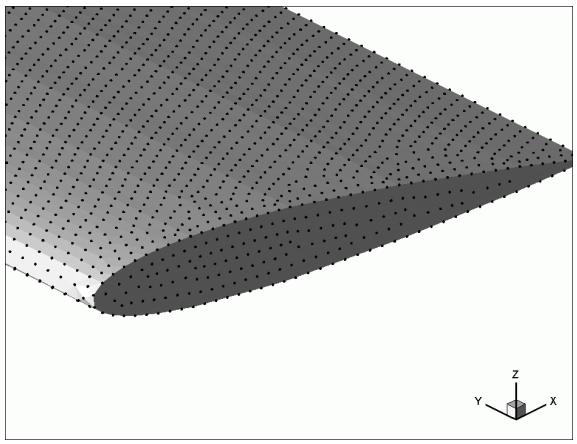

Figure 2: The surface of an airfoil NACA-0012 characterized by Lagrangian points.

The main characteristic of Immersed Boundary method is to simulate the presence of a fluid/solid or fluid/fluid interface inside a flow by adding a source term of force $\vec{f}$ to the Navier-Stokes equations. In Fig. (3) an arbitrary Lagrangian point k is shown with coordinates $\vec{x}_k$, as well as an elementary volume of fluid with coordinates $\vec{x}$. The evaluation of $\vec{f}$ differentiates the IB methods among them.

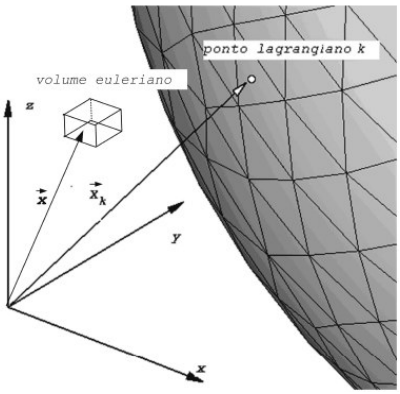

Figure 3: Schematic drawing of an arbitrary point k over a surface, placed on $\vec{x}_k$, and a element of fluid positioned in $\vec{x}$

In the Virtual Physical Model, the Lagrangian force is obtained from a balance of momentum over a particle k, placed at $\vec{x}_k$. This particle also has properties pressure p_k and velocity $\vec{V}_k$. Thus, the force can be evaluated as:

$$\vec{F}_k = \frac{\partial(\rho \vec{V}_k)}{\partial t} + \vec{\nabla}\cdot(\rho \vec{V}_k \vec{V}_k) - \mu \nabla^2 \vec{V}_k + \vec{\nabla} p_k \tag{3}$$

The Eq. (3) can be interpreted as the necessary force so that a particle of fluid immediately adjacent to the Lagrangian point k reaches the velocity of this point, imposing a non-slip condition between the fluid and the immersed body.

Each term of the Eq. (3) has a particular meaning. The first term (the transient term) is responsible by the acceleration force ($\vec{F}_{acc}$). The other terms, of spatial derivatives, are known as the advective term, the diffusive term and the pressure gradient term, respectively. These terms are responsible for inertial forces ($\vec{F}_{inert}$), viscous forces ($\vec{F}_{visc}$), and pressure forces ($\vec{F}_{press}$). More details about this model and about each term evaluation can be found in Lima e Silva et al (Lima e Silva *et al*, 2003), and Campregher (2005).

The properties of the flow in the Eulerian mesh have to be interpolated to the Lagrangian mesh to calculate the Lagrangian forces. Once evaluated, the Lagrangian forces must be transferred back to the Eulerian domain. The connection between Lagrangian and Eulerian domains is promoted by the force distribution procedure.

2.2.1. The Virtual Physical Model

The discretization of Eq (3) is done by constructing a three-dimensional reference axis, with origin placed at the point k, as can be seen in the Fig (4). A Lagrangian polynomial is then used to obtain the space derivatives along each coordinate direction. Let *m* be a number of points employed to construct a polynomial interpolation of order *m-1*. Thus, the value of a property ϕ along *i* direction, at any point p, is given by:

$$\phi_i(p) = \sum_m \psi_m(p)\phi_m \,, \tag{4}$$

where,

$$\psi_m(p)i = \prod_{n,n\neq m}\left[\frac{x_i(p) - x_i(n)}{x_i(p) - x_i(n)}\right]. \tag{5}$$

Substituting the *m* points, according to the stencil on Fig (4), the ϕ property value along the *x* axis (where k, k_1 and k_2 points lay) can obtained as:

$$\phi_p = \left[\frac{(x_p - x_{k1})(x_p - x_{k2})}{(x_k - x_{k1})(x_k - x_{k2})}\right]\phi_k + \left[\frac{(x_p - x_k)(x_p - x_{k2})}{(x_{k1} - x_k)(x_{k1} - x_{k2})}\right]\phi_{k1} + \left[\frac{(x_p - x_k)(x_p - x_{k1})}{(x_{k2} - x_k)(x_{k2} - x_{k1})}\right]\phi_{k2}. \tag{6}$$

Deriving Eq (6) to *x* direction one has:

$$\frac{\partial \phi_p}{\partial x} = \left[\frac{(x_p - x_{k1}) + (x_p - x_{k2})}{(x_k - x_{k1})(x_k - x_{k2})}\right]\phi_k + \left[\frac{(x_p - x_k) + (x_p - x_{k2})}{(x_{k1} - x_k)(x_{k1} - x_{k2})}\right]\phi_{k1} + \left[\frac{(x_p - x_k) + (x_p - x_{k1})}{(x_{k2} - x_k)(x_{k2} - x_{k1})}\right]\phi_{k2}, \tag{7}$$

and the second derivative results:

$$\frac{\partial^2 \phi_p}{\partial x^2} = \left[\frac{2\phi_k}{(x_k - x_{k1})(x_k - x_{k2})}\right] + \left[\frac{2\phi_{k1}}{(x_{k1} - x_k)(x_{k1} - x_{k2})}\right] + \left[\frac{(x_p - x_k) + (x_p - x_{k1})}{(x_{k2} - x_k)(x_{k2} - x_{k1})}\right]. \tag{8}$$

From the equations above, it is possible to obtain every spatial derivative needed in Eq (3), just substituting the point *p* and the aimed variable ϕ.

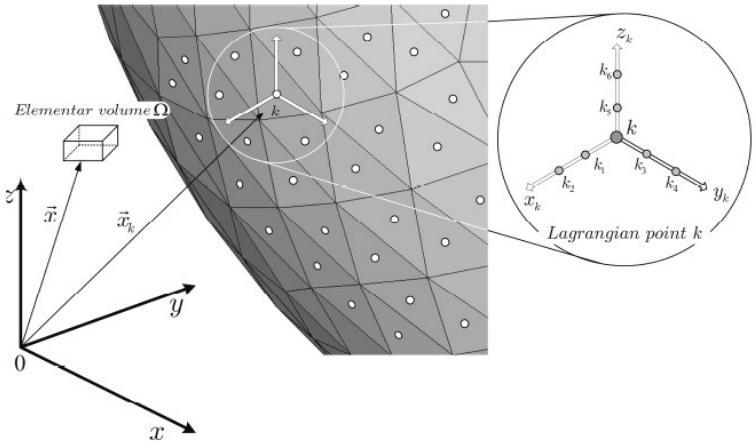

Figure 4: Position of the Lagrangian point $\vec{x}_k$

A detailed view of a triangular element can be obtained in the Fig (5). The element sides are formed by line segments S_1, S_2, and S_3, between the vertex points P_1, P_2 and P_3. Thus, one has $S_1 = \overline{P_2 P_1}$, $S_2 = \overline{P_3 P_2}$ and $S_3 = \overline{P_3 P_1}$.

The ΔA_k is the triangular element surface area, which can be evaluated as:

$$\Delta A_k = \sqrt{S(S - S_1)(S - S_2)(S - S_3)} \tag{9}$$

where $S = (1/2)(S_1 + S_2 + S_3)$. The ΔS_k is the average length of the triangle sides. It worth noting that each of those geometric properties are associated to a Lagrangian point *k*.

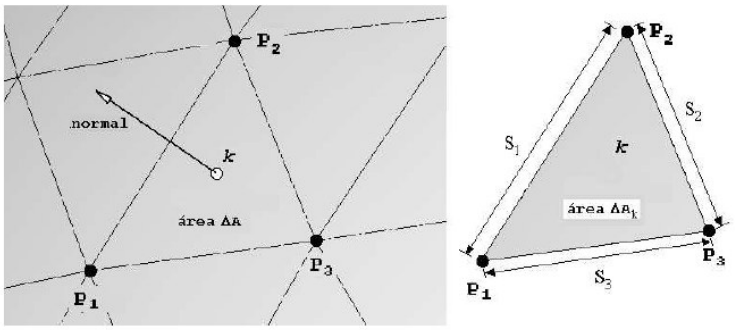

Figure 5: Detailed view of a triangular element

2.2.2. The distribution procedure

The Lagrangian force term $\vec{F}$, calculated at a Lagrangian point (denoted by Ω_k) is then distributed to Eulerian domain by means of the Dirac Delta Function. In a N-dimensional this function is defined as:

$$\vec{f}(\vec{x}) = \int_{R^n} \delta(\vec{x} - \vec{x}_k)\vec{F}(\vec{x}_k)d^n\vec{x}_k \quad . \tag{10}$$

Applying the Eq. (10) for a volume V of the Lagrangian domain,

$$\vec{f}(\vec{x}) = \int_{\Omega_n} \vec{F}(\vec{x}_k)\delta(\vec{x} - \vec{x}_k)d\vec{x}_k \quad . \tag{11}$$

The δ function has the following property:

$$\int_{R^n} \delta(\vec{x} - \vec{x}_k)d\vec{x} = \begin{cases} 1 & if\ \vec{x}_k \in V \\ 0 & if\ \vec{x}_k \notin V \end{cases}, \tag{12}$$

where $V \in \Omega$ .This function acts as the core of a transformed integral (centered in $\vec{x}_k$), which promotes the transposition between the Lagrangian and Eulerian domains (Griffith and Peskin, 2005).

In the Virtual Physical Model for three-dimensional domains, the Lagrangian force field ($F_{i,k}$) is distributed over the Eulerian mesh using Eq (13).

$$f_i = \sum F_{i,k} D_i \Delta A_k \Delta S_k \quad . \tag{13}$$

The distribution function D_i is evaluated as:

$$D_i(x_k) = \prod_i \left\{ \frac{\varphi[(x_k - x_i)/\Delta x_i]}{\Delta x_i} \right\}, \tag{14}$$

where the φ function is defined as:

$$\varphi(r) = \begin{cases} \tilde{\varphi}(r) & if\ \|r\| < 1 \\ \frac{1}{2} - \tilde{\varphi}(2-r) & if\ 1 < \|r\| < 2 \\ 0 & if\ \|r\| > 2 \end{cases}, \tag{15}$$

$$\tilde{\varphi}(r) = \frac{3 - 2\|r\| + \sqrt{1 - 4\|r\| + 4\|r\|^2}}{8}. \tag{16}$$

The Distribution function is divided by a volume unit, that cancel out by multiplying for a characteristic area (ΔA_k) and for a characteristic length (ΔS_k). Thus, it remains the force density that is integrated over the volume Ω .

The interface solid/fluid is managed by an indicator function I_i , built from:

$$\nabla^2 I_i = \nabla G_i , \tag{17}$$

where the *G* function is defined as:

$$G_i = \sum D_i \vec{n}_k \Delta A_k , \tag{18}$$

and the $\vec{n}_k$ is the normal vector on the Lagrangian point k.

After the discretization of the Eq. (17), the algebraic equation system is evaluated by the MSI algorithm (Schneider and Zedan, 1981), a variation of the SIP procedure. By analyzing the Eq. (18), one can see that if the geometry is inserted into a non-uniform grid region, the interfacial region may become deformed, i.e., the geometry shell shape would be misrepresented.

Briefly describing, the force field evaluation procedure in the Virtual Physical Model can be stated as:

(1) With the flow field solved, the velocity components and the pressure are transferred, using the interpolation function given by Eq. (18), to the nearest Lagrangian points *(k, k1...k6)* depicted in Fig. (4);

(2) Once having $u_{i,k}$ and $p_{i,k}$, evaluates $F_{i,k}$ by Eq. (3);

(3) Calculates the force field components, due to each Lagrangian point k, via Eq. (13);

(4) Advances in time;

(5) The force field are inserted into the source-term of Eq. (1);

(6) A new flow field is obtained and the procedure re-starts.

3. Parallel Programming Approach

One of the greatest problems involving complex physical problems simulations is the computational resources available. Thus, an in-house Beowulf cluster turns out to be very a viable solution due to its comparatively low cost when comparing to the supercomputers. Moreover, such clusters have good scalability, that is, it is possible to increase the cluster resource by adding more processors anytime. The cheaper assembly is ensured by employing on-the-shelf hardware and, mainly, due to the open source software, freely downloaded from internet.

Any group of ordinary machines connected by a local network may be enough to constitute a Beowulf cluster. This work ran on a homogeneous cluster of five machines with the following configurations: master node has an Intel® 865PERL mother-board, a Pentium4® 2.8GHz processor, with 1548 MB DDR RAM, 80 GB IDE hard drive, and a Radeon® 9200 128MB DDR AGP8x video card. The slave nodes have the same configuration, except by the video card, which is a Geforce® 64MB AGP4x. The postprocessing tasks are done by master node. All machines are connected by a Gigabit network via 3COM® 16 port switch.

The software uses for data interchange among processors the MPI (Message Passage Interface) library, more specifically a MPICH (MPI CHameleon). The MPI was chosen, mainly, due to its better performance on clusters of homogeneous machines. Furthermore, the MPI library has more than 120 functions permitting to write very efficient codes and, also, it is constantly updated by the MPI community.

The computational domain was split in 3 sub-domains with the Lagrangian mesh entirely in one of them, since it is not parallelized yet. Furthermore, as described above, it is imperative to use uniform spacing grids within and over the immersed geometry region. The other regions of the Eulerian domain was discretized in a non-uniform mesh to save computational resources. The way the problem was partitioned can be seen in fig. (6).

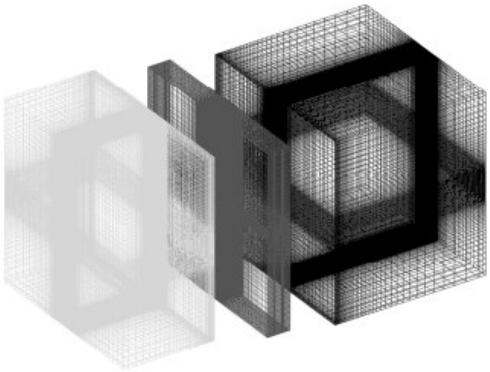

Figure 6: Eulerian sub-domains used in the simulations.

4. Results and discussion

Craft (Craft et al, 2006) studied the formation and decay of wingtip vortices based on experimental results obtained by Chow (Chow et al, 1997). Those papers were used to qualitatively validate the present work.

The numerical Eulerian mesh used for every simulation is detailed in the Fig (7). The numerical domain has dimensions *length (X)* = 0.88*m*, *width (Y)* = 0.68 *m* and *height (Z)* = 0.336 *m.* Such domain was discretized by, 148x268x76 grids in *X*, *Y* and *Z* axis, respectively.

The NACA 0012 airfoil is represented by a triangular element mesh, as seen in Fig. (8), composed by 15446 nodes and 30888 elements. Again, the Immersed Boundary methodology requires only the discretization of the surface that represents the fluid/solid interface, i.e. the body shell. The airfoil is centered at (x_c, y_c, z_c) = (*0.28, 0.34, 0.165) m*, having a chord *c=0.04m* and a width of 4*c*. For every simulation the attack angle $\alpha = 10^o$ and the Reynolds number, based on chord, is Re = 10000.

The boundary condition for velocity components on the Eulerian domain side walls were set as free-slip conditions, the inflow at *x=0 m* had a flat profile with values of $u = U_1$ (inlet velocity), $v = w = 0 m/s$. The outflow was set of Neumann conditions.

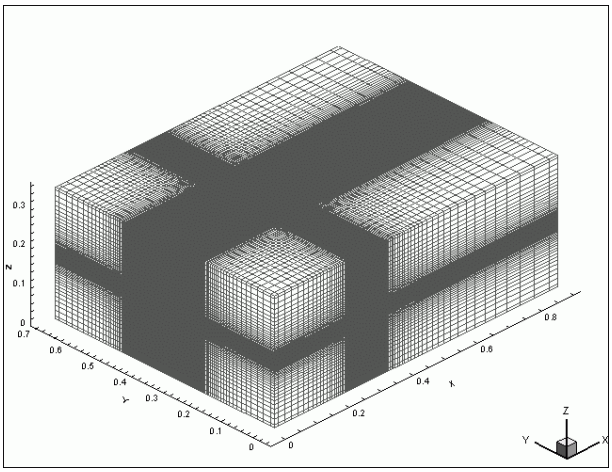

Figure 7: Eulerian and Lagrangian domain.

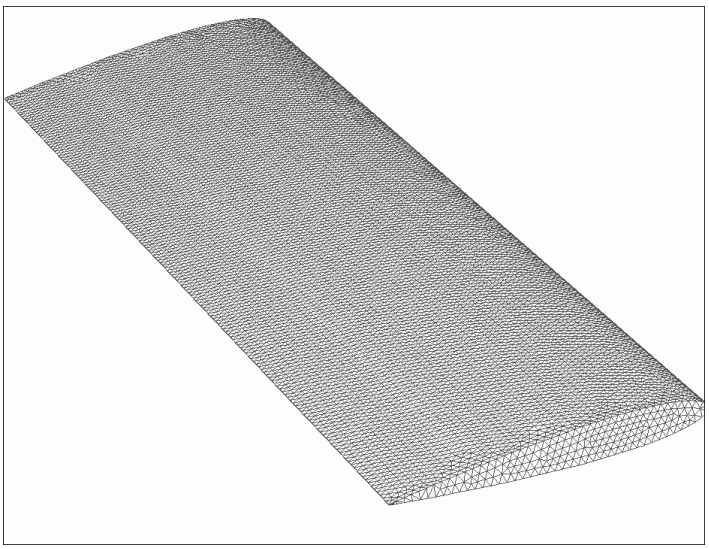

Figure 8: Airfoil discretized using a triangular elements mesh.

Computations are here reported as the flow over a NACA 0012 airfoil with a square wing tip. The generation and the evolution on time of the trailing vortices are well shown for a low Reynolds number (Re = 10000).

In Figs (9a-h) it is possible to see the formation and evolution of the streamlines over the NACA 0012 airfoil of Fig (8). Since the overall flow pattern is symmetric at this flow regime, only one side of the airfoil is shown.

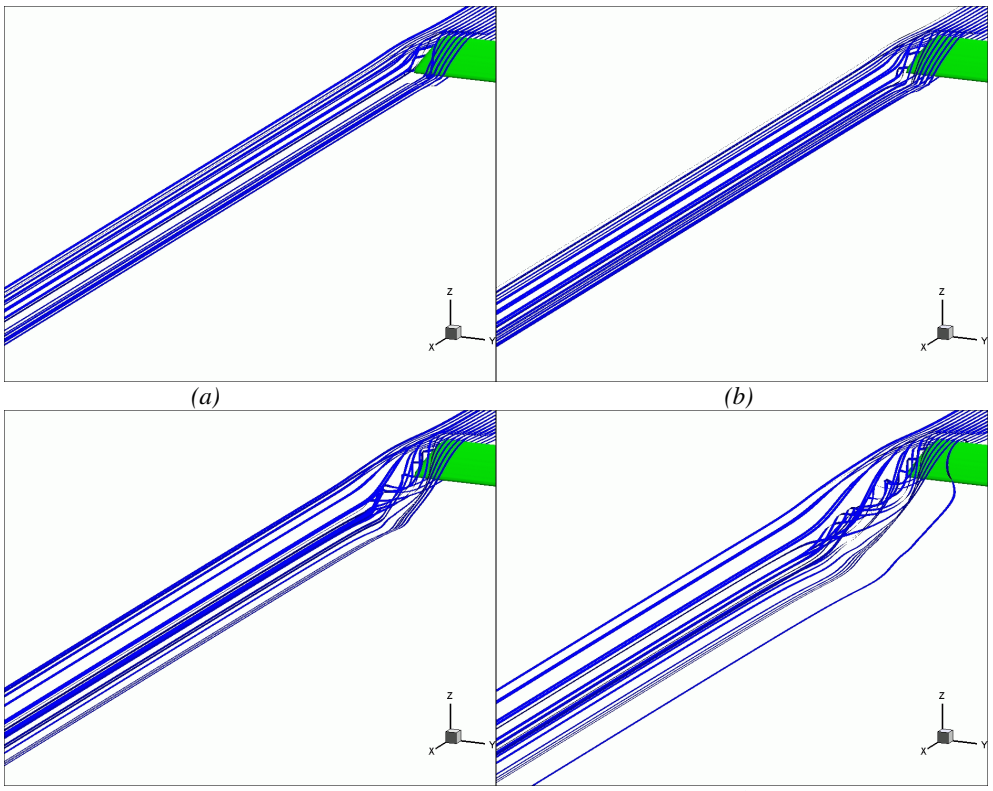

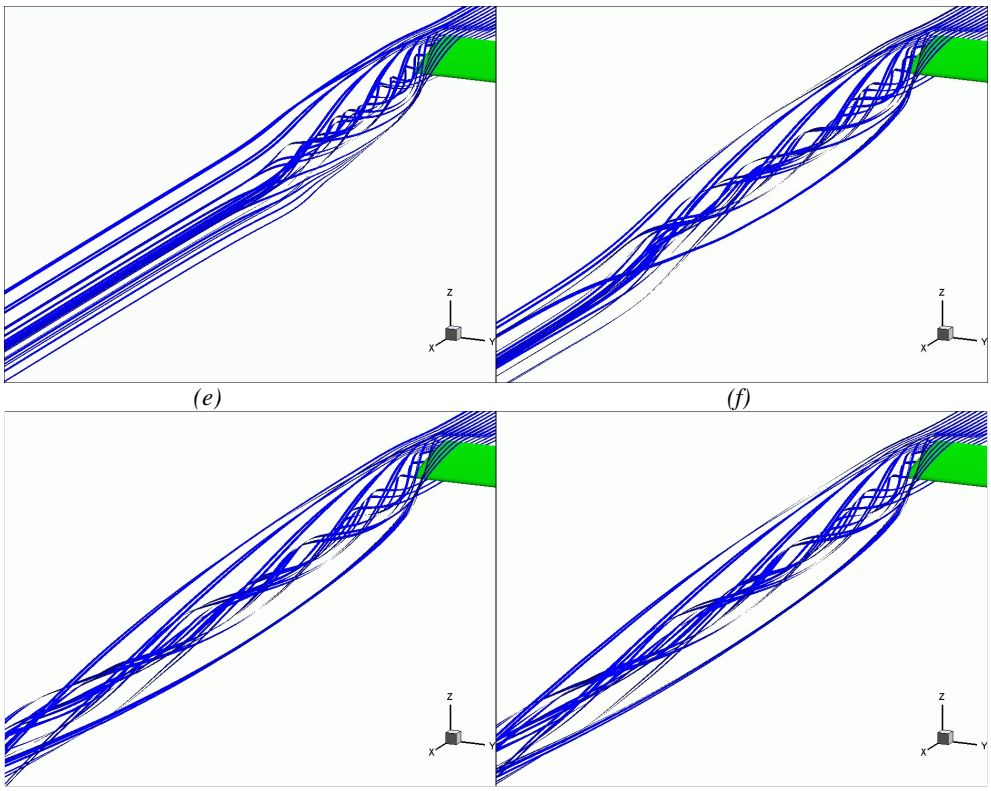

(e) *(f)*

(g) *(h)*

Figure 9: Evolution of streamlines over an NACA 0012 airfoil on times: *(a) t=0.01s, (b) t=0.1s (c) t=0.5s (d) t=1.0s (e) t=1.5s (f) t=3.0s (g) t=5.0s (h) t=10.0s.*

The value of the L2 norm was about $10^{-3,}$ which is acceptable, once that the code has a second order in time-space accuracy.

Figure (10) shows three perpendicular planes to the airfoil. It's notable the influence of the tip of wing on the flow. We see that the flow is symmetric, and at the airfoil middle a Kelvin-Helmholtz like instability is formed and it is being transported. Figure (11) and Fig (12), show the top view and the back view of Fig (10). At Fig (12) the helicoidal wingtip vortices are clearly shown.

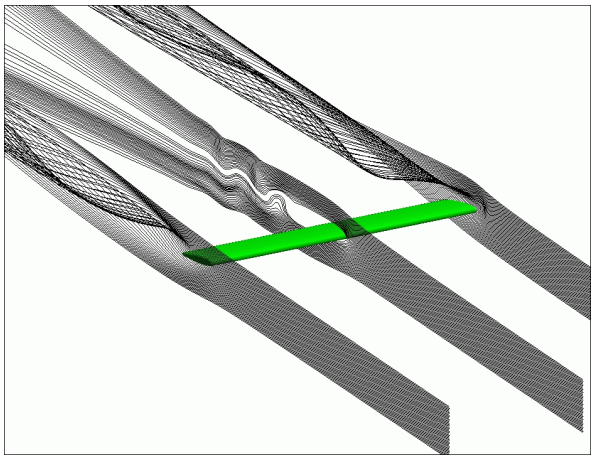

Figure 10: Perpendicular planes at *t=10.0s*.

Figure 11: Top view of Fig. 10

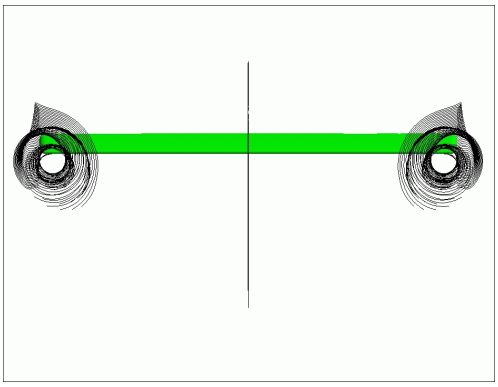

Figure 12: Back view of Fig 10.

In Figs (13a-f), the vorticity field is shown over six transversal cuts. It's possible to see the formation and evolution of the vertical structures over the NACA 0012 airfoil.

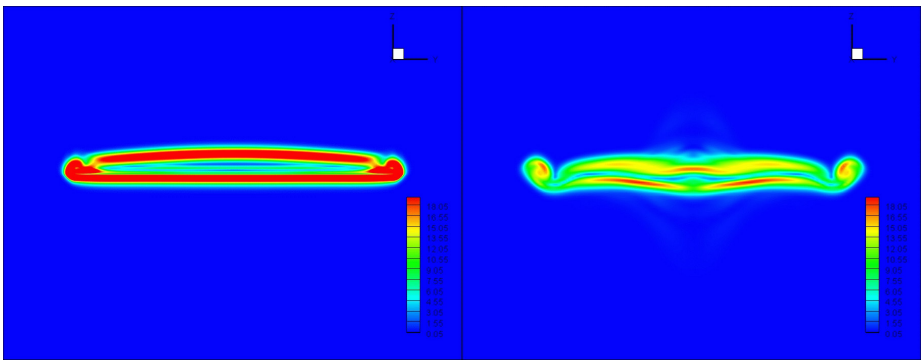

(a) *(b)*

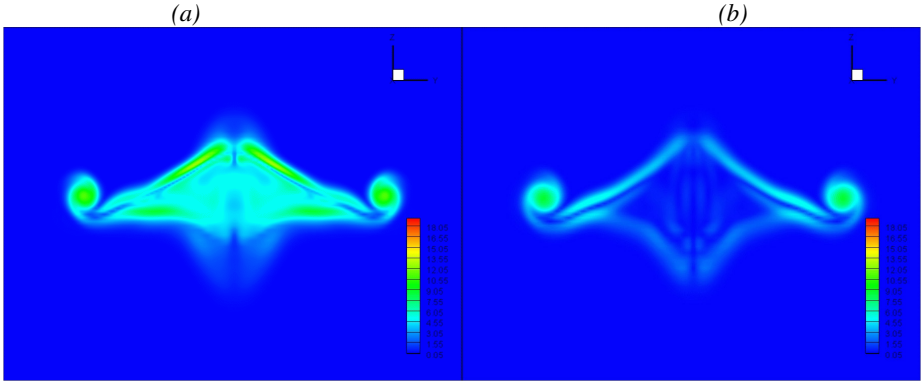

(c) *(d)*

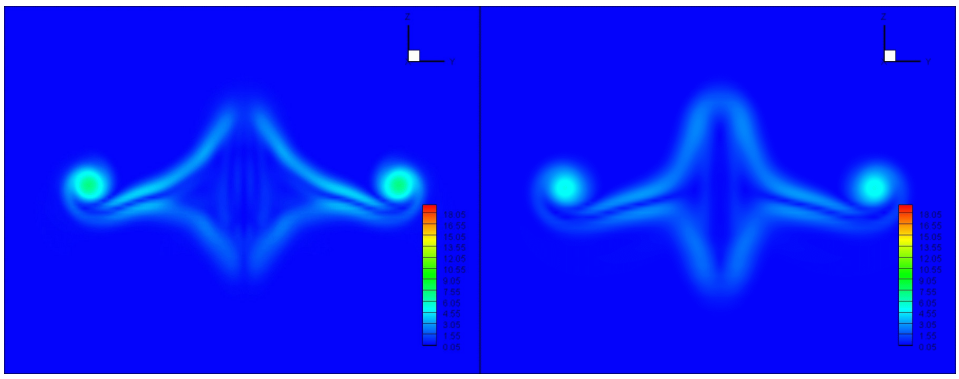

(e) *(f)*

Figure 13: Evolution of the vorticity field behind the airfoil in *t=10s* at positions: *(a) x=0.3m, (b) x=0.34m (c) x=0.4m (d) x=0.45m (e) x=0.5m (f) x=0.6m*

In Fig (13) it is possible to note that the main structure that remains in the flow are the vortices generated by the tip of the airfoil. From this result, it can be said that those structures are really matter of concern, when studying large aircrafts.

5. Conclusion

In this work, which represents an extension of Campregher's work (Campregher, 2005), the authors intended to present more applications to Virtual Physical Method. The flow around a single airfoil NACA 0012 at *Re = 10000* was chosen as a test case to identify and characterize the generation and the decay of wingtip vortices. It was done successfully.

The Immersed Boundary Method have shown great capability in dealing with complexes geometries and/or moving bodies, once the Eulerian mesh is a Cartesian mesh, very simple to be created, and there are no further difficulties in generating the Lagrangian mesh, which is a advantage if compared with other methodologies of studying Fluid-Structure Interaction.

The results present a good agreement with literature (Chow et al, 1994 and Craft et al, 2006), and also, it is possible to understand the generation and development of the vortices. Although, further investigation about the influence of the width of the airfoil in the flow, as well as development for high Reynolds number have to be done.

6. References

Campregher, Rubens, Modelagem Matemática tridimensional para problemas de interação fluido-estrutura, doctoral thesis, Uberlândia 2005

Chow, J.S., 1994. Turbulence measurements in the near-wake of a wingtip vortex. Thermosciences Division Rep. No. MD-69, Mechanical Engineering Department, Stanford University.

Craft, T.J.; Gerasimov, A.V.; Launder, B.E.; Robinson C.M.E.; A computational study of the near-field generation and decay of wingtip vortices. International Journal of Heat and Fluid Flow, 2006

Ferziger J and Peric M., Computational methods for fluid dynamics 3th ed., 2002, Springer-Verlag, New-York, USA.

Griffith, B. e Peskin, C., 2005, "On the order of accuracy of the immersed boundary method: Higher order convergence rates for sufficiently smooth problems.", Journal of Computational Physics 208, 75-105.

Lima e Silva A.L.F., Silveira-Neto, A., and Damasceno, J.J.R; Numerical simulation of two dimensional flows over a circular cylinder using the immersed boundary method, J. Comp. Phys. 189, 351 (2003)

Mohd-Yusof, J. Combined immersed boudaries/B-splines methods for simulations in complex geometries, CTR Annual Research Briefs, NASA Ames/Stanford University, 1997.

Muzaferija, S. e Peric, M., 1997, "Computational of free-surface flows using the Finite-Volume method and moving grids", Numerical Heat Transfer, Part B 32, 369-384.

Peskin C.S., Numerical analysis of the blood flow in the heart, J. Comp. Phys. 25, 220 (1977)

Rhie C. and Chow W., Numerical study of turbulent flow past an airfoil with trailing edge separation, AIAA Journal 21, 1525 (1983)

Schneider G.E. and Zedan M., A modified strongly implicit procedure for the numerical solution of field problems, Numer. Heat Transfer 4, 1 (1981)

Van Doormal, J. e Raithby, G., "Enhancements of the simple method for predicting incompressible fluid flows", Numerical Heat Transfer 7, 147-163, 1984